Available online at www.sciencedirect.com

ScienceDirect

Ceramics International 40 (2014) 3975–3979

CERAMICS INTERNATIONAL

www.elsevier.com/locate/ceramint

Simple fabrication of rod-like N-doped TiO_2/Ag with enhanced visible-light photocatalytic activity

Xiufeng Zhou, Juan Lu, Jialei Cao, Mengfei Xu, Zuoshan Wang*

College of Chemistry, Chemical Engineering and Materials Science, Soochow University, Soochow 215123, China

Received 23 July 2013; accepted 8 August 2013
Available online 16 August 2013

Abstract

Rod-like N-doped TiO_2/Ag composites were successfully synthesized by a modified sol–gel method, without adding any surfactants. The entire preparation differs from the traditional sol–gel synthesis of TiO_2 that the reaction can get controlled by adjusting the flow speed of water vapor and NH_3. Characterization results show that as-prepared samples were uniform nanorods with an average length of ca. 3 μm and a cross section diameter of ca. 150 nm. The rod-like structure was formed during the annealing process. A possible mechanism was proposed to illustrate the formation of rod-like Ag–N–TiO_2. The degradation of methylene blue performed under visible light with the prepared nanorods as the photocatalyst demonstrated the photocatalytic activities of TiO_2 can be improved by the synergistic effect of N doping and Ag modification. In addition, as-prepared TiO_2-based photocatalyst exhibits a significantly enhanced photo-chemical stability after 5 catalytic cycles mainly due to the rod-like morphology. This indicated that they have some potential value in practical application.

Keywords: A. Grain growth; B. Nanocomposites; C. Chemical properties; D. TiO_2

1. Introduction

TiO_2 has been widely used in various fields including photocatalysis [1], lithium batteries [2], sensors [3] as well as solar cells [4], due to its unique and favorable physico-chemical properties. Recently, a considerable number of studies have proved that compared with TiO_2 particles, rod-like TiO_2 takes many advantages, such as easy separation and high recycle rate, which make it more suitable for practical applications [5–7]. So far, several methods have been used to fabricate rod-like TiO_2 including the assisted-template method [8], electrochemical anodic oxidation [9] and hydrothermal treatment [5].

Besides, nano-TiO_2 also has some limitations in the use of solar energy, such as a wide energy band gap and fast recombination rate of charge carriers [1,4]. Since Asahi et al. reported the synthesis of $TiO_{2-x}N_x$ film with an enhanced visible light absorption [10], N doping has been considered as an effective way to improve the photocatalytic activity of nano-TiO_2. Previous reports also proved that Ag modification could eliminate the recombination of electron–hole pairs effectively [11]. However, there are few reports related to the synthesis of TiO_2 modified with Ag and doped with N simultaneously. It is reasonable to expect the N-doped TiO_2/Ag composites will show a superior photocatalytic activity under visible light irradiation.

Herein, rod-like N-doped TiO_2/Ag composites were fabricated by a modified and facile sol–gel approach. Ammonia was used as the source of N and H_2O, and the rod-like structure was formed during the annealing process, which differs from the reported fabrication of C–N co-doped TiO_2 nanorods [12]. The reaction is controllable by adjusting the flow speed of water vapor and NH_3. As-prepared samples have a uniform particle size, and exhibit an excellent photocatalytic activity and stability under visible light.

2. Experimental procedure

2.1. Preparation of rod-like N-doped TiO_2/Ag

In all experiments, deionized water was used. All of the chemical were analytical grade.

*Corresponding author. Tel./fax: +86 0512 85187680.
E-mail address: zuoshanwang@suda.edu.cn (Z. Wang).

0272-8842/$ - see front matter
http://dx.doi.org/10.1016/j.ceramint.2013.08.045

In a typical synthesis, 8 mL of tetrabutyl titanate (TBOT) and 40 mL of ethanol were mixed together in a flask. An air blower connected with a round bottom flask containing 300 mL ammonia (5 wt%) was turned on to transport air at a rate of 40 L min^{-1}. A small quantity of NH_3 along with water vapor was carried into the reaction flask with the air to react with the mixture. The TBOT solution hydrolyzed slowly to form a cream color emulsion under ceaseless stirring for 30 min. Then 0.034 g of $AgNO_3$ was dissolved in 10 mL of ethanol and was added dropwise to the emulsion. Reaction stopped after 15 min, and then the emulsion was dried in a drying oven and irradiated under UV light for 15 min. The precursor was annealed at 400 °C for 2 h to prepare the rod-like N-doped TiO_2/Ag composite, designated as Ag–N–TiO_2. As a comparison, pure TiO_2 (TiO_2), N-doped TiO_2 (N–TiO_2) and Ag-loaded TiO_2 (Ag–TiO_2) were also synthesized by a similar way.

2.2. Characterization of the samples

The crystalline phase identification and structural analysis were done by X-ray diffraction (XRD) instrument with Cu-Kα radiation. A USA Thermo ESCALAB 250 X-ray photoelectron spectrometer (XPS) was applied to analysis the elemental composition and state of samples. The microstructures were analyzed by scanning electron microscopy (SEM) and transmission electron microscopy (TEM). The UV–vis diffuse reflectance spectra of the samples were characterized using a Japan Shimadzu UV240 UV–vis spectrophotometer.

2.3. Photocatalytic activity

The photocatalytic activity was evaluated by degradation of methylene blue (MB) under visible light using as-prepared samples as the photocatalyst. Detailed procedures can be found in our previous report [12]. The actual effect of photocatalytic activity by chemical reaction was studied by maintaining the solutions in dark for 1 h before irradiation to reach the adsorption–desorption balance. The degradation rate of MB can be calculated via the formula $\eta=(1-A_i/A_0)\times 100\%$, where A_0 is the absorbance of original MB solution before irradiation, and A_i is the absorbance of MB solution measured every 5 min. The photodegradation of MB follows pseudo-first-order kinetics. Its kinetics can be expressed as $\ln(C_0/C)=kt$, where k (h^{-1}) is the degradation rate constant.

The stability of photocatalyst was evaluated by the degradation of MB with reused photocatalyst, and the same amount of new MB solution was used each time.

3. Results and discussion

Fig. 1 shows the typical XRD patterns of as-prepared samples. Several diffraction peaks that can be assigned to the anatase phase are unambiguously identified (JCPDS no. 21-1272). Neither silver nor nitrogen-derived peaks could be detected in all of the samples, mainly due to the low dosage of the dopant well dispersed in TiO_2 particles [13,14]. The

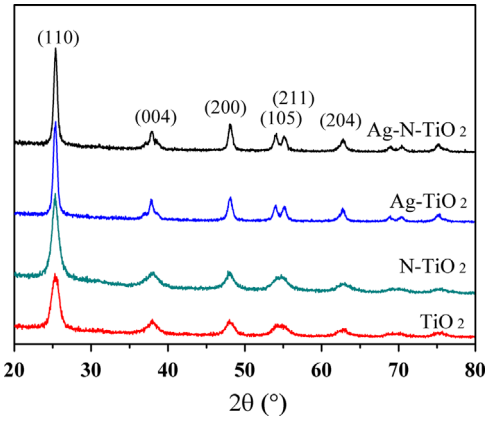

Fig. 1. XRD patterns of different samples.

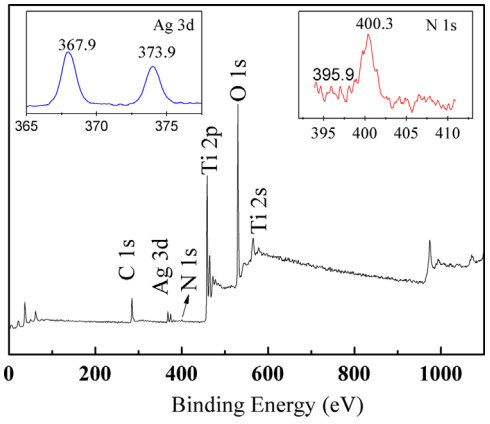

Fig. 2. XPS spectra of the sample Ag–N–TiO_2.

average sizes of the samples (TiO_2, N–TiO_2, Ag–TiO_2 and Ag–N–TiO_2) were respectively 6.7 nm, 7.1 nm, 14.2 nm and 16.4 nm, calculated with the Scherrer formula.

The XPS results of the sample Ag–N–TiO_2 is shown in Fig. 2, and the binding energies obtained in the XPS analysis are corrected for specimen charging by referencing C ls to 285 eV. The peaks observed in this spectrum are assigned to C, O, Ti, N, and Ag. The insets display the high-resolution peaks of N 1s and Ag 3d. The N 1s spectrum reveals two peaks located at 400.3 eV and 395.9 eV, which can be attributed to nitrogen species bound to various surface oxygen sites (NO-like species) [15] and the Ti–N bond resulting from the substitution of nitrogen atoms for oxygen sites in the TiO_2 lattice [16], respectively. The binding energies of 367.9 eV and 373.9 eV in the Ag 3d spectrum were attributed to Ag $3d_{5/2}$ and Ag $3d_{3/2}$, respectively. The splitting of the Ag 3d doublet is 6.0 eV, indicating that Ag is of metallic nature in our samples [17]. A detailed quantitative analysis indicates that the atomic concentration of C, O, Ti, N and Ag in the samples is 18.65%, 58.3%, 22.47%, 0.34%, and 0.24%, respectively. The excess oxygen and carbon atoms were ascribed to the absorption of O_2 and CO_2 on the surface of the samples.

The SEM and TEM images of as-prepared samples are shown in Fig. 3. It can be observed that the sample Ag–N–TiO_2 after annealing became uniform nanorods with an average length

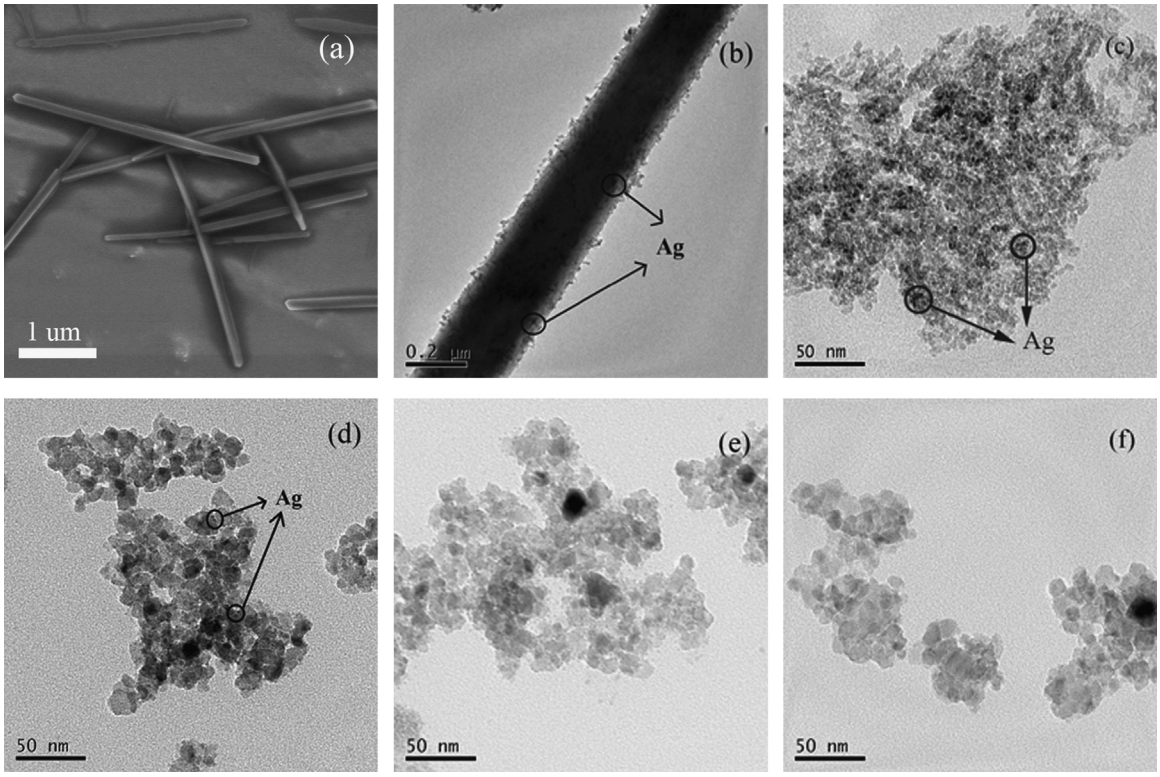

Fig. 3. (a) and (b) SEM and TEM images of Ag–N–TiO_2 after annealing; (c) TEM image of Ag–N–TiO_2 before annealing; (d)–(f) TEM images of Ag–TiO_2, N–TiO_2 and TiO_2, respectively, after annealing.

of ca. 3 μm and a cross section diameter of ca. 150 nm, while it was nanoparticle with a diameter of about 5 nm before annealing, indicating annealing has an important influence on the morphology of the samples. In addition, the samples TiO_2, N–TiO_2 and Ag–TiO_2 obtained after annealing were all nanoparticles with diameters of about 20 nm, which implied that the formation of rod-like N-doped TiO_2/Ag composite is mainly due to the synergistic effect of N and Ag during the annealing process. Another obvious phenomenon was that a few less bright spots existed on the surface of Ag–TiO_2, Ag–N–TiO_2 before annealing and Ag–N–TiO_2 after annealing as displayed in Fig. 3b–d, correspond to the homogenously dispersed Ag nanoclusters [18], which is consistent with the XPS results mentioned above.

On the basis of the SEM observations of the samples at different annealing periods (as shown in Fig. 4), a possible mechanism was proposed to illustrate the formation of rod-like Ag–N–TiO_2.

(i) Formation of random rice-like nanoparticles. During the initial stage of annealing, many rice-like nanoparticles were formed through the dehydration reaction (Fig. 4(b)). These rice-like nanoparticles trend to arrange randomly to lower their surface energy.
(ii) Oriented self-assembly. From the point of view of crystal growth, the formation of many small crystals is kinetically favored, (i.e. they nucleate more easily) but large crystals are thermodynamically favored [19]. As the annealing time extends, as-formed particles aggregate to form wicker-like nanoparticles to attain a lower energy state (Fig. 4(c)). With the annealing going on, wicker-like nanoparticles connected one another on their high energy plane. As a result, the rod is loosely packed with some wicker-like nanoparticles on the surface (Fig. 4(d)).
(iii) Further growth. As known to all, small crystals have a larger surface area to volume ratio than large crystals. Molecules on the surface are energetical, and thus they are less stable than the ones already well ordered and packed in the interior. Thus, many small crystals on the surface will attain a lower energy state if transformed into large crystals (Ostwald ripening). The transformation can result in the formation of rod-like Ag–N–TiO_2 with smooth surfaces (Fig. 4(e and f)).

UV–vis diffuse reflectance spectra, as shown in Fig. 5, revealed that the samples N–TiO_2 and Ag–TiO_2 exhibited a wider and stronger absorption of visible light than that of TiO_2. In addition, rod-like N-doped TiO_2/Ag exhibited a significant absorption of both ultraviolet and visible light, suggesting that doping TiO_2 with N and modifying it with Ag simultaneously made its band gap narrowed, which is beneficial to the improvement of the photocatalytic efficiency.

Fig. 6(a) displays the photo-catalytic degradation of MB solution under visible irradiation using as-prepared samples as the photo-catalysts. It can be observed that after irradiation for 3 h, about 97% of the MB solution has been degraded using the rod-like N-doped TiO_2/Ag as a photocatalyst, while under

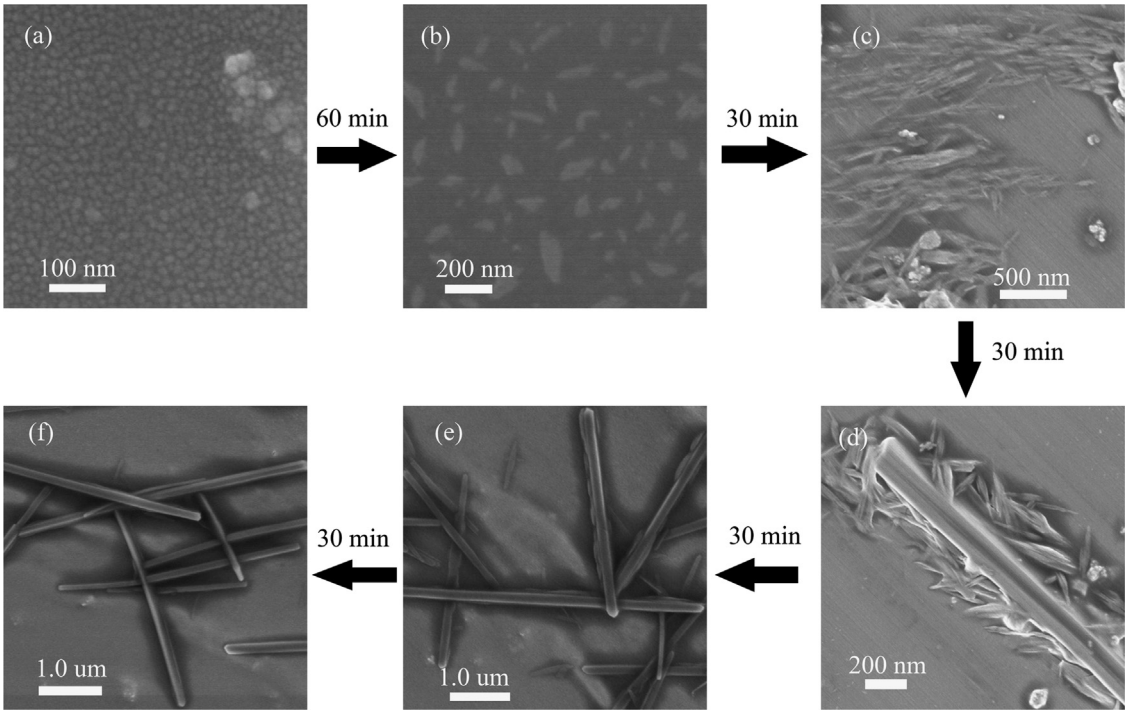

Fig. 4. The growth mechanism of rod-like Ag–N–TiO_2.

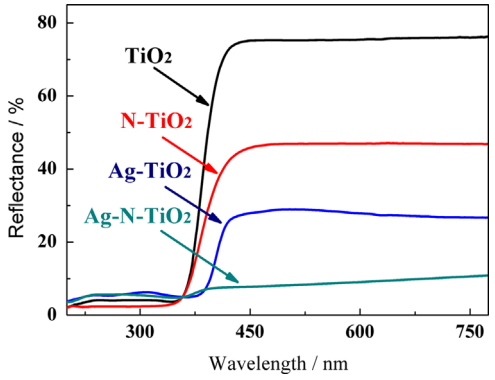

Fig. 5. UV–vis reflectance spectra of as-prepared samples.

the same conditions, only about 80%, 79% and 57% of the solution can be degraded using respectively Ag–TiO_2, N–TiO_2 and TiO_2 as the photo-catalyst, leading to a conclusion that as-prepared rod-like N-doped TiO_2/Ag composite has a remarkably enhanced photocatalytic activity mainly due to the synergistic effect of N doping and Ag modification.

Fig. 6(b) shows a linear relationship between $\ln(C_0/C)$ and reaction time, indicating that the photodegradation of MB follows first-order kinetics. The apparent rate constants were determined as 0.29, 0.51, 0.54 and 1.02 h^{-1} for TiO_2, N–TiO_2, Ag–TiO_2 and rod-like N-doped TiO_2/Ag, respectively. The order of rate constants is summarized as follows: TiO_2 < N-TiO_2 < Ag–TiO_2 < N-doped TiO_2/Ag, which is consistent with the conclusions of photocatalytic degradation curves presented in Fig. 6(a).

To evaluate the stability of these photo-catalysts, the repeated experiments for the degradation of MB were performed using TiO_2, N–TiO_2, Ag–TiO_2 and Ag–N–TiO_2 as the catalysts, and the results are shown in Fig. 7. The activity of TiO_2, N–TiO_2 and Ag–TiO_2 decreased dramatically after 5 catalytic cycles. In contrast, the reused Ag–N–TiO_2 maintained high catalytic activities. In detail, 97% of MB could be degraded within 3 h when Ag–N–TiO_2 is used for the first time, and the proportion decreased to 91% after 5 recycles. Therefore, the synergistic effect of N doping and Ag modification plays an important role in improving the stability of TiO_2-based photocatalyst. Besides, the photocatalyst with the rod-like morphology can be separated and recycled more easily than that with the nanoparticle morphology, which is another important factor in the high stability of Ag–N–TiO_2.

4. Conclusions

In summary, the N-doped TiO_2/Ag composites have been successfully fabricated by a modified sol–gel approach, without any surfactants. Characterization results show that as-prepared samples were uniform nanorods with an average length of ca. 3 μm and a cross section diameter of ca. 150 nm. The rod-like structure was formed during the annealing process. Compared with TiO_2, N–TiO_2 and Ag–TiO_2, the rod-like N-doped TiO_2/Ag composites exhibit a significantly improved photocatalytic activity under visible light and maintain high photo-chemical stability after 5 catalytic cycles, mainly due to the synergistic effect of N doping and Ag modification. In addition, the rod-like morphology also plays an important role in improving the stability of the TiO_2-based photocatalyst.

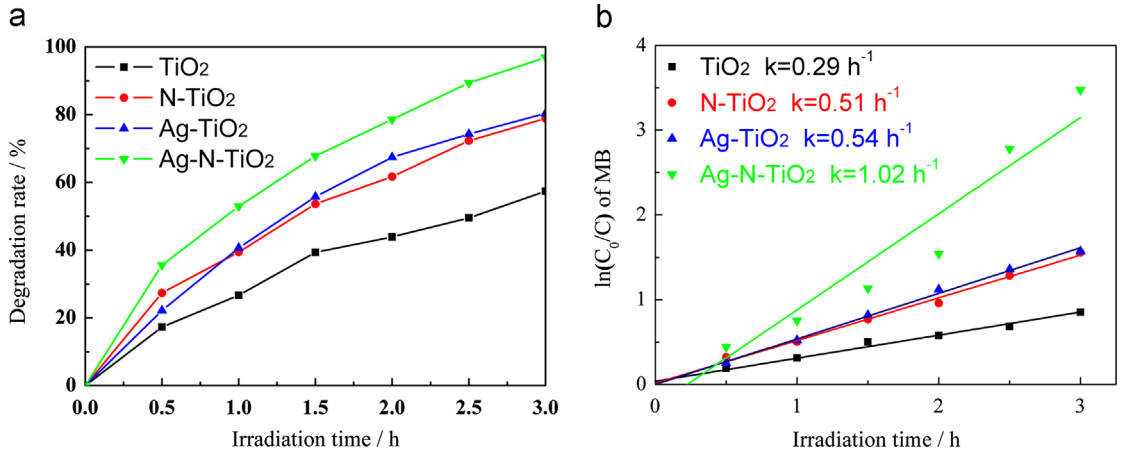

Fig. 6. (a) The degradation curves of MB under visible light irradiation; (b) the plot of $\ln(C_0/C)$ with irradiation time of visible light for different samples.

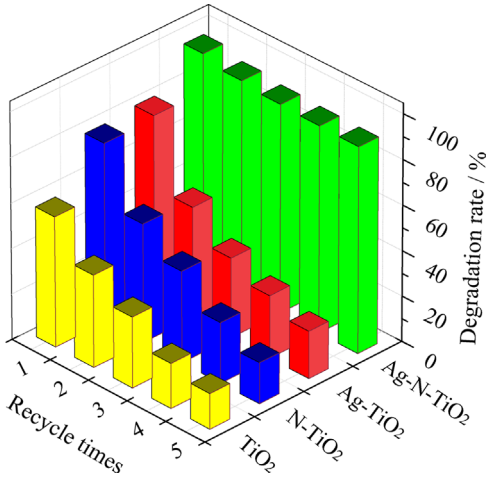

Fig. 7. Photochemical stability of as-prepared samples.

Acknowledgments

The authors are grateful for the financial support of a project funded by the Priority Academic Program Development of Jiangsu Higher Education Institutions.

References

[1] H. Li, W. Zhang, W. Pan, Enhanced photocatalytic activity of electrospun TiO_2 nanofibers with optimal anatase/rutile ratio, Journal of the American Ceramic Society 94 (2011) 3184–3187.

[2] G. Armstrong, A.R. Armstrong, P.G. Bruce, P. Reale, B. Scrosati, TiO_2 (B) nanowires as an improved anode material for lithium-ion batteries containing $LiFePO_4$ or $LiNi_{0.5}Mn_{1.5}O_4$ cathodes and a polymer electrolyte, Advanced Materials 18 (2006) 2597–2600.

[3] G. Wang, Q. Wang, W. Lu, J. Li, Photoelectrochemical study on charge transfer properties of TiO_2-B nanowires with an application as humidity sensors, Journal of Physical Chemistry B 110 (2006) 22029–22034.

[4] K. Zhu, N.R. Neale, A. Miedaner, A.J. Frank, Enhanced charge-collection efficiencies and light scattering in dye-sensitized solar cells using oriented TiO_2 nanotubes arrays, Nano Letters 7 (2007) 69–74.

[5] C. Xiong, X. Deng, J. Li, Preparation and photodegradation activity of high aspect ratio rutile TiO_2 single crystal nanorods, Applied Catalysis B: Environmental 94 (2010) 234–240.

[6] N. Li, L. Zhu, W. Zhang, Y. Yu, W. Zhang, M. Hou, Modification of TiO_2 nanorods by Bi_2MoO_6 nanoparticles for high performance visible-light photocatalysis, Journal of Alloys and Compounds 509 (2011) 9770–9775.

[7] Z. Wu, F. Dong, W. Zhao, H. Wang, Y. Liu, B. Guan, The fabrication and characterization of novel carbon doped TiO_2 nanotubes, nanowires and nanorods with high visible light photocatalytic activity, Nanotechnology 20 (2009) 235701–235709.

[8] J.H. Jung, H. Kobayashi, K.J.C. van Bommel, S. Shinkai, T. Shimizu, Creation of novel helical ribbon and double-layered nanotube TiO_2 structures using an organogel template, Chemistry of Materials 14 (2002) 1445–1447.

[9] Z. Zhang, Yuan, G. Shi, Y. Fang, L. Liang, H. Ding, et al., Photoelectrocatalytic activity of highly ordered TiO_2 nanotube arrays electrode for azo dye degradation, Environmental Science and Technology 41 (2007) 6259–6263.

[10] R. Asahi, T. Morikawa, T. Ohwaki, K. Aoki, Y. Taga, Visible-light photocatalysis in nitrogen-doped titanium oxides, Science 293 (2001) 269–271.

[11] P.V. Kamat, Photophysical, photochemical and photocatalytic aspects of metal nanoparticles, Journal of Physical Chemistry B 106 (2002) 7729–7744.

[12] L. Li, J. Lu, Z. Wang, L. Yang, X. Zhou, L. Han, Fabrication of the CN co-doped rod-like TiO_2 photocatalyst with visible-light responsive photocatalytic activity, Materials Research Bulletin 47 (2012) 1508–1512.

[13] X. Li, X. Zou, Z. Qu, Q. Zhao, L. Wang, Photocatalytic degradation of gaseous toluene over Ag-doping TiO_2 nanotube powder prepared by anodization coupled with impregnation method, Chemosphere 83 (2011) 674–679.

[14] L. Lin, R.Y. Zheng, J.L. Xie, Y.X. Zhu, Y.C. Xie, Synthesis and characterization of phosphor and nitrogen co-doped titania, Applied Catalysis B: Environmental 76 (2007) 196–202.

[15] L. Zhao, Q. Jiang, J.S. Lian, Visible-light photocatalytic activity of nitrogen-doped TiO_2 thin film prepared by pulsed laser deposition, Applied Surface Science 254 (2008) 4620–4625.

[16] X. Yang, C. Cao, L. Erickson, K. Hohn, R. Maghirang, K. Klabunde, Synthesis of visible-light-active TiO_2-based photocatalysts by carbon and nitrogen doping, Journal of Catalysis 260 (2008) 128–133.

[17] M. Wu, B. Yang, Y. Lv, Z. Fu, J. Xu, T. Guo, et al., Efficient one-pot synthesis of Ag nanoparticles loaded on N-doped multiphase TiO_2 hollow nanorod arrays with enhanced photocatalytic activity, Applied Surface Science 256 (2010) 7125–7130.

[18] G. Li, H. Liu, H. Zhao, Y. Gao, J. Wang, H. Jiang, et al., Chemical assembly of TiO_2 and TiO_2@ Ag nanoparticles on silk fiber to produce multifunctional fabrics, Journal of Colloid and Interface Science 358 (2011) 307–315.

[19] Y. Sang, B. Geng, J. Yang, Fabrication and growth mechanism of three-dimensional spherical TiO_2 architectures consisting of TiO_2 nanorods with {110} exposed facets, Nanoscale 2 (2010) 2109–2113.